

Received: 2017.03.31  
Accepted: 2017.05.09  
Published: 2017.05.27

# MicroRNAs Correlate with Multiple Sclerosis and Neuromyelitis Optica Spectrum Disorder in a Chinese Population

Authors' Contribution:  
Study Design A  
Data Collection B  
Statistical Analysis C  
Data Interpretation D  
Manuscript Preparation E  
Literature Search F  
Funds Collection G

**BDF 1,2** **Jianglong Chen**  
**BD 1** **Jiting Zhu**  
**CD 3** **Zeng Wang**  
**BD 2** **Xiaoping Yao**  
**BD 1** **Xuan Wu**  
**DF 1** **Fang Liu**  
**B 4** **Weidong Zheng**  
**AD 1** **Zhiwen Li**  
**ADEG 1** **Aiyu Lin**

1 Department of Neurology, The First Affiliated Hospital of Fujian Medical University, Fuzhou, Fujian, P.R. China  
2 Department of Neurology, Jinjiang Hospital of traditional Chinese Medicine, Jinjiang, Fujian, P.R. China  
3 Department of Neurology, The Third Affiliated Hospital of Fujian Medical University, Fuzhou, Fujian, P.R. China  
4 Department of Ophthalmology, Jinjiang Hospital of Traditional Chinese Medicine, Jinjiang, Fujian, P.R. China

**Corresponding Authors:** Aiyu Lin, e-mail: 15359181549@163.com, Zhiwen Li, e-mail: lc1985929@126.com

**Source of support:** This work was funded by the Key Research Project of Science and Technology Office of Fujian Province (Grant No. 2014Y022)

**Background:** Recent studies identified a set of differentially expressed miRNAs in whole blood that may discriminate neuromyelitis optica spectrum disorders (NMOSD) from relapsing-remitting multiple sclerosis (RRMS). This study invalidated 9 known miRNAs in Chinese patients.

**Material/Methods:** The levels of miRNAs in whole blood were assayed in healthy controls (n=20) and patients with NMOSD (n=45), RRMS (n=17) by quantitative real-time polymerase chain reaction (qRT-PCR), and pairwise-compared between groups. They were further analyzed for association with clinical features and MRI findings of the diseases.

**Results:** Compared with healthy controls, miR-22b-5p, miR-30b-5p and miR-126-5p were down-regulated in NMOSD, in contrast, both miR-101-5p and miR-126-5p were up-regulated in RRMS. Moreover, the levels of miR-101-5p, miR-126-5p and miR-660-5p, were significantly higher in RRMS than in NMOSD (P=0.04, 0.01 and 0.02, respectively). The level of miR-576-5p was significantly higher in patients underwent relapse for ≤3 times than those for ≥4 times. In addition, its level was significantly higher in patients suffered from a severe visual impairment (visual sight ≤0.1). Moreover, the levels of each of the 9 miRNAs were lower in NMOSD patients with intracranial lesions (NMOSD-IC) than those without (NMOSD-non-IC). Despite correlations of miRNAs with these disease subtypes, all AUCs of ROC generated to discriminate patients and controls, as well as intracranial lesions, were <0.8.

**Conclusions:** Certain miRNAs are associated with RRMS and NMOSD. They are also related to the clinical features, especially intracranial lesions of NMOSD. However, none of the miRNAs alone or in combination was powerful to ensure the diagnosis and differentiation of the 2 disease subtypes.

**MeSH Keywords:** **MicroRNAs • Multiple Sclerosis • Neuromyelitis Optica**

**Full-text PDF:** <http://www.medscimonit.com/abstract/index/idArt/904642>

 2857

 5

 3

 34



## Background

Multiple sclerosis (MS) and neuromyelitis optica spectrum disorders (NMOSD) are autoimmune demyelinating disorder of the central nervous system. Only a few biomarkers are available in the clinical practice, such as cerebrospinal fluid oligoclonal bands and serum anti-aquaporin 4 antibodies. Thus, there is a significant unmet need for biomarkers to assess diagnosis and prognosis. MicroRNAs, a kind of small non-coding RNA present in stable form in the human blood, have attracted much attention as novel diagnostic biomarkers for many diseases, such as tumors and autoimmune diseases [1]. Functionally, these miRNAs regulate gene expression involving cell division, metabolism, stress response, and angiogenesis [2–5]. Others play roles in proliferation, invasion and migration of cancer [6–10].

Previous studies demonstrated that miRNA expression profiles in whole blood or purified blood cell subtypes are correlated with MS and that circulating miRNAs are differentially expressed in different stages of MS [11–14], making them easily accessible for monitoring MS [15]. Moreover, recent study identified a set of differentially expressed miRNAs in whole blood that may discriminate neuromyelitis optica spectrum disorders (NMOSD) from relapsing-remitting multiple sclerosis (RRMS) in Europeans [16]. However, there are less reports on the correlation between miRNAs and clinical features and pathology of NMOSD. For instance, it is unclear how certain miRNAs contribute specifically to brain pathology in NMOSD.

So far there is no accurate epidemiological data on NMOSD worldwide, but it is well known that NMOSD accounts for a much higher proportion of idiopathic inflammatory demyelinating diseases (IIDDs) (40%) in Asians than in white populations (1%) [17]. Regarding a predominance of NMOSD in Chinese and remarkable differences of clinical features and genetic backgrounds between Eastern and Western populations [18], we sought to re-evaluate the correlation of these miRNAs with NMOS and RRMS Chinese. We also analyzed the association of these miRNAs with the clinical features of these diseases.

## Material and Methods

### Patients

A total of 62 patients were diagnosed and treated in The First Affiliated Hospital of Fujian Medical University from November 2013 to July 2016. Twenty healthy adults (18 females, 2 males, aged  $44.7 \pm 9.8$  years) were recruited as normal controls. Among all the cases, 45 were diagnosed as NMOSD according to 2015 International Consensus Diagnostic Criteria for Neuromyelitis Optica Spectrum Disorders [18], and 17 were diagnosed with

RRMS according to the McDonald 2010 criteria [19] and 2016 MRI criteria for the diagnosis of multiple sclerosis: MAGNIMS consensus guidelines [20]. We defined patients within 8 weeks after an acute attack with NMOSD or RRMS as active phase, more than 8 weeks as a stable phase according to the diagnostic criteria for MS [14].

All clinical information including MRI and laboratory tests were collected and evaluated by senior neurologists with expertise in neuroimmunology. The clinical features of the 3 categories of patients were listed in Table 1. The 2 patient groups were significantly different in age and female preponderance. Among 40 NMOSD patients who underwent anti-AQP4 antibody detection by cell-based transfection immunofluorescence assay (CBA, EUROIMMUM Medical Diagnostic, China Co. Ltd.), 34 (85.0%) were positive, the other 5 patients who did not make detection were diagnosed by AQP4 negative diagnostic criteria. Among 10 RRMS patients underwent anti-AQP4 antibody detection, none was positive. The proportion of B lymphocyte in peripheral blood mononuclear cells (PBMCs) was detected in 23 NMOSD patients, among which 8 were decreased and 12 were increased. 15 of 36 NMOSD patients underwent other autoantibodies detection, including ANA, ANA spectrum, dsDNA, ACA, AnCA, and 15 (41.7%) were positive. Among 15 RRMS patients underwent autoantibodies detection, 1 (6.7%) was positive. Parenchymal lesions were found in 19 (42.2%) NMOSD cases among which 14 (31.1%) met the neuroimaging criteria of the 2015 International Consensus Diagnostic Criteria for Neuromyelitis Optica Spectrum Disorders and 2016 MRI criteria for the diagnosis of multiple sclerosis: MAGNIMS consensus guidelines. These lesions located extensively in the brain regions, including medulla oblongata and area postrema (6/14), midbrain (2/14), thalamus (1/14), periaqueductal, lateral ventricle and the third ventricle (3/14), corpus callosum (3/14) and cerebral hemisphere (4/14). All NMOSD cases received 500–1000 mg of methyl prednisolone treatment in acute stage, which were gradually reduced to 10mg as maintenance dosage for 3 to 36 months. Thirteen patients were treated with gamma globulin 400 mg/kg intravenous injection for 5 days together with prednisolone in the acute phase. Twelve cases used azathioprine 100–150 mg/day for 3 to 60 months, and 3 of them also used cyclosporine 100–150 mg/day for 12 to 36 months. This study was approved by the Ethics Committee of The First Affiliated Hospital of Fujian Medical University (ID: clinical research 2014y0022) and written informed consent was obtained from all study participants.

### Selection of miRNAs for measurement

A total of 9 miRNAs were selected for verification in our study, including miR-15b-3p (chr3: 160404588-160404685), miR-22b-5p (chr5: 13813148-13813229), miR-30b-5p (chr8: 134800520-134800607), miR-101-5p (chr1: 65058434-65058508),

**Table 1.** Clinical features of the studied subjects.

Clinical feature	NMOSD (n=45)	RRMS (n=17)	CIS (n=14)	HC (n=20)	P value		
					NMOSD vs. RRMS	NMOSD vs. HC	RRMS vs. HC
Female/male ratio	6.5:1	1.4:1	2.5:1	9:1	0.02	0.53	0.08
Age at study (year)	40.9±12.8	31.2±9.3	46.4±17.3	44.7±9.8	0.01	0.25	0.06
Age at onset (year)	36.1±13.3	28.9±8.1	44.4±17.3	–	0.04		–
Disease duration (year)	4.9±6.6	3.8±4.6	1.8±5.3	–	0.49		–
Relapse (time)	3.4±2.1	2.2±0.9	–	–	0.03		–
EDSS score at the last visit	3.4±2.0	2.4±1.1	2.4±1.2	–	0.06		–
Ratio of visual impairment (≤0.1/>0.1)	9:36	1:16	6:8	–	0.17		–
Ratio of anti-AQP4-Ab positivity (±)	34/6	0/10	0/5	–	<0.0001		–
Ratio of autoantibody positivity (±)	15/21	1/14	0/10	–	0.002		–

miR-126-5p (chr9: 136670602-136670686), miR-223-5p (chrX: 66018870-66018979), miR-335-3p (chr7: 130496111-130496204), miR-576-5p (chr4: 109488698-109488795) and miR-660-5p (chrX: 50013241-50013337). All of them showed significantly different expression levels in both NMOSD vs. CIS/RRMS and NMOSD vs. healthy controls in whole blood according to the Keller's study [23].

#### Peripheral blood RNA isolation and qRT-PCR

A 5-ml blood sample was collected in EDTA tubes from each of the participants and stored at –80°C. MiRNAs was extracted from peripheral whole blood using Tri-Reagent (Life Technologies) according to the manufacturer's instructions. The purity and concentration of RNA were determined using NanoDrop One (Thermo Scientific). For quantitative detection of miRNA by RT-PCR, purified whole blood miRNA was converted to cDNA by reverse transcription reactions using TaqMan MicroRNA Reverse Transcription Kit (Applied Biosystems) and miRNA-specific stem-loop primers were supplied by the TaqMan MicroRNA Assays (Applied Biosystems).

Selected miRNAs were measured by quantitative real-time reverse transcription polymerase chain reaction (RT-PCR) using the qPCR Master Mix (Promega) and QuantStudio® 5 Real-Time PCR System (Applied Biosystems) according to the manufacturer's instructions. The reactions were incubated in a 96-well optical plate at 95°C for 5 min, followed by 40 cycles at 95°C for 15 s, and 60°C for 40 s. Reactions were performed in triplicate. The cycle threshold (CT) was recorded, which was defined as the number of PCR cycles required for the fluorescent signal to be higher than a threshold indicating baseline variability. Cel-miR-39-3p was chosen as the exogenous reference

control. Amplification and melting working curves of all miRNAs are shown in Supplementary Figures 1 and 2. Relative changes of miRNA expression were represented by 2-ΔCT.

#### Bioinformatics analysis

We used the miEAA ([http://www.ccb.uni-saarland.de/mieaa\\_tool/](http://www.ccb.uni-saarland.de/mieaa_tool/)) as a tool to characterize the association of the miRNAs with molecular pathways. MiEAA is based on GeneTrail [24] and used for standard enrichment analyses, such as over-representation analysis or gene set enrichment analysis in the context of miRNAs. Adjusted *p* values <0.05 were considered significant enrichment.

#### Statistical analysis

Numeric data were expressed as mean ± standard deviation (SD). Statistical analyses were performed using the professional statistical computer software, GraphPad Prism 5. Differences between groups were tested using the one-way ANOVA rank test or two-tailed student t-test, *P*<0.05 for two-tailed test was set as the level of statistical significance. Post hoc testing was carried out between the samples. The *P* values were corrected by the Tukey-Kramer standard.

## Results

#### Clinical features of the NMOSD and RRMS patients

Clinical features of the patients with NMOSD, RRMS are listed in Table 1 and compared with healthy controls (HCs). Compared to RRMS, NMOSD patients had older onset (*P*=0.04), more

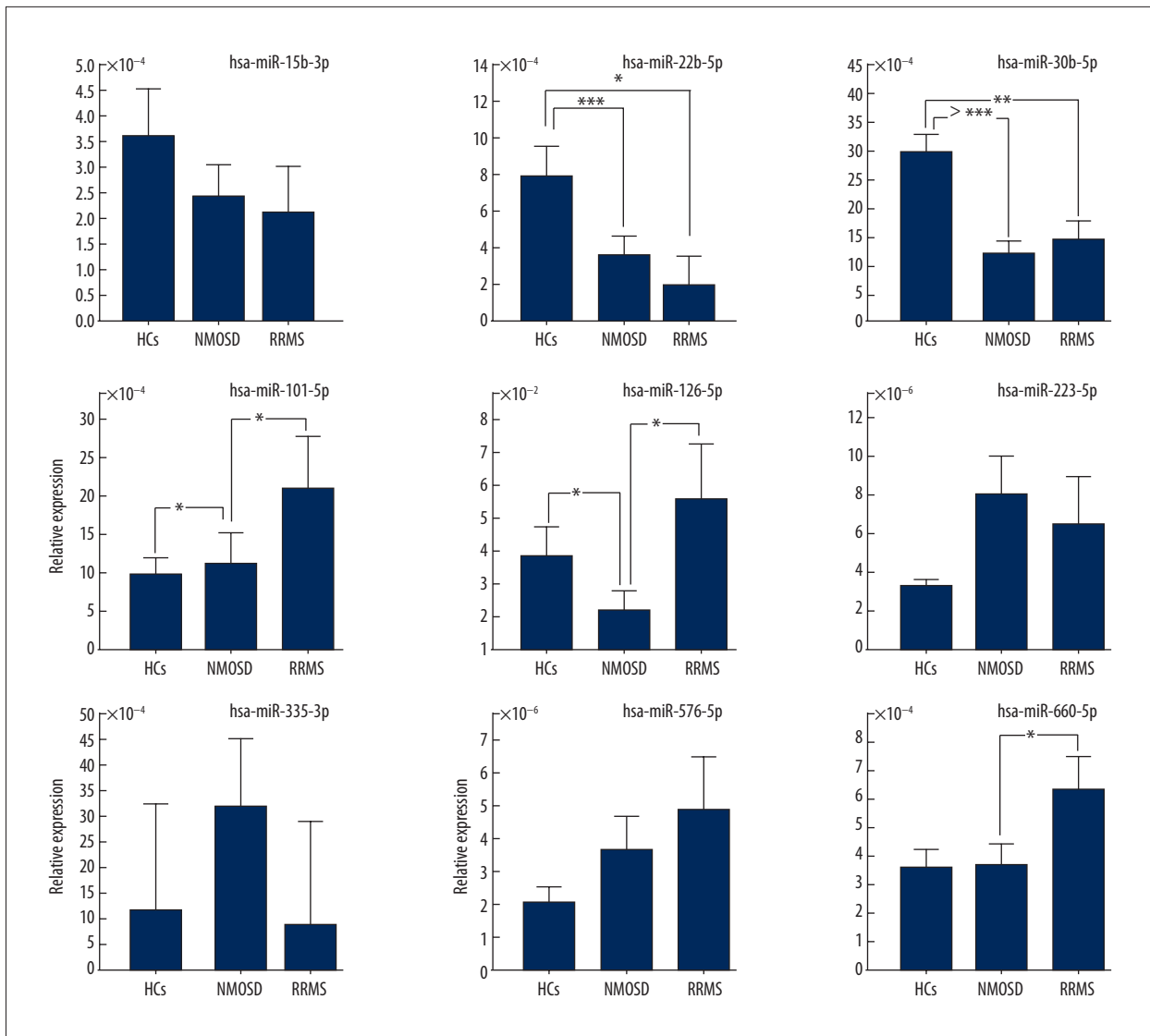


**Figure 1.** The expression level of the 9 miRNAs in HCs, NMOSD and RRMS separately, as well as the statistical significance among all groups. NMOSD – neuromyelitis optica spectrum disorders; RRMS – relapsing-remitting multiple sclerosis; HCs – healthy controls. NMOSD (n=45), MS (n=17), HCs (n=20). The bar diagram shows the mean 2-ΔCT values and standard deviations. \* P<0.05, \*\* P <0.01, \*\*\* P<0.001.

significant female preponderance (P=0.02), higher frequency of recurrence (P=0.03), as well as higher positive rate of anti-AQP4 antibody (P<0.0001) and autoantibody (P=0.002).

**Alterations of the miRNA expression level in NMOSD and RRMS**

The levels of all measured miRNAs are shown in Figure 1. As compared with healthy controls (HCs), miR-22-5p, miR-30b-5p and miR-126-5p were down-regulated in NMOSD (P=0.02, P<0.001 and P=0.04, respectively). In contrast, miR-101-5p and miR-126-5p were expressed at higher levels in RRMS (P=0.03 and P=0.04) than in controls. Moreover, the levels

of miR-101-5p, miR-126-5p as well as miR-660-5p, were significantly higher in RRMS than in NMOSD (P=0.04, 0.01 and 0.02, respectively).

**Correlation between miRNA levels and the clinical features of NMOSD**

Based on a significant correlation between miRNAs with the development of NMOSD, we next analyzed the correlation between miRNA expression level and clinical features of NMOSD, including age, gender, disease duration, recurrence times, severity of visual impairment, EDSS score, AQP4 antibody titers, proportion of B lymphocyte subsets, and MRI findings.

**Table 2.** Correlation between miRNA expression and the clinical features of NMOSD.

Clinical features	Categorized comparisons	miR-15b-3p	miR-22-5p	miR-30b-5p	miR-335-3p	miR-101-5p	miR-126-5p	miR-223-5p	miR-576-5p	miR-660-5p
		P	P	P	P	P	P	P	P	P
Gender	Female (n=39) vs. Male (n=6)	0.93	0.89	0.84	0.09	0.51	0.71	0.48	0.67	0.78
Phase of clinical course	Active (n=30) vs. stable (n=15)	0.27	0.09	0.26	0.1	0.83	0.71	0.92	0.65	0.36
Times of relapse	≤3 (n=25) vs. ≥4 (n=20)	0.67	0.34	0.09	0.87	0.44	0.3	0.05	<b>0.01</b>	0.08
EDSS score	≤3 (n=23) vs. >3 (n=22)	0.5	0.81	0.52	0.39	1	0.62	0.55	0.48	0.21
Visual impairment	Yes (n=18) vs. No (n=27)	0.85	0.74	0.63	0.55	0.28	0.99	0.49	0.16	0.37
	≤0.1 (n=9) vs. >0.1 (n=36)	0.53	0.49	0.84	0.78	0.21	0.99	<b>0.04</b>	<b>0.003</b>	0.06
AQP4-Ab(titre)	Negative (n=6) vs. Positive (n=34)	0.71	0.47	0.65	0.44	0.32	0.48	0.4	0.48	0.7
	≤1: 32 (n=20) vs. ≥1: 100 (n=20)	0.23	0.39	0.11	0.49	0.51	0.25	0.95	0.72	0.86
Autoantibody	Positive (n=14) vs. Negative (n=20)	0.52	0.31	0.94	0.77	0.43	0.17	0.8	0.44	0.44
MRI enhancement	Positive (n=13) vs. Negative (n=32)	0.31	0.26	0.14	0.18	0.09	0.21	0.49	0.5	0.22
Spinal cord involved (segment)	<6 (n=17) vs. >6 (n=19)	0.36	0.38	0.23	0.62	0.59	0.91	0.68	0.64	0.66
B lymphocyte prootion (%)	<9.0 (n=8) vs. >14.1 (n=12)	0.29	0.28	0.66	0.36	0.35	0.6	0.56	0.57	0.63

By comparing the miRNA levels in patients displaying each of the two-categorized clinical features, we found that the level of miR-576-5p was significantly higher in patients underwent relapse for ≤3 times than those for ≥4 times (P=0.01). In addition, its level was significantly higher in patients suffered from a severe visual impairment (visual sight ≤0.1) (P=0.003). Similar changes were revealed in the level of miR-223-5p in patients with more relapses and visual impairment, but with lower statistical significance (P=0.05 and 0.04, respectively). There was no significant correlation between the expression level of the remaining 7 miRNAs and the NMOSD features (Table2).

#### Correlation between miRNAs with intracranial lesions in NMOSD patients

The demyelinating lesions in CNS of NMOSD are mainly confined within the optic nerve and spinal cord. However, it has been demonstrated that intracranial (IC) lesions are also common, and that different molecular mechanisms may account for cases with and without intracranial. Thus, we asked whether

this difference may be related to miRNAs. To address this, we further divided the NMOSD patients into 2 subgroups, showing typical intracranial (IC) and without (non-IC) lesions according to MRI findings, and compared the miRNA levels of patients in RRMS patients. Among 45 NMOSD cases, 14 (31.1%) had typical intracranial lesions distributed widely in the white matters, including paraventricular, subcortical regions and corpus callosum. As shown in Figure 2, the levels of each of 9 miRNAs were lower in NMOSD patients with intracranial lesions (NMOSD-IC) than those without (NMOSD-non-IC). In addition, although the level of miR-15b-3p, miR-22b-5p, miR-30b-5p and miR-126b-5p were reduced in NMOSD as a whole, they were only significantly down-regulated in the NMOSD-IC subgroup, as compared with HCs. Similarly, only the NMOSD-IC patients showed lower miR-15b-3p, miR-30b-5p, miR-223-5p and miR-576b-5p levels than the NMOSD-non-IC patients. Interestingly, the level of miR-15b-5p was significantly lower in the NMOSD-IC patients than in RRMS and HCs, although its level in all NMOSD patients was not significantly different from patients with these groups (Figure 1). In contrast, there

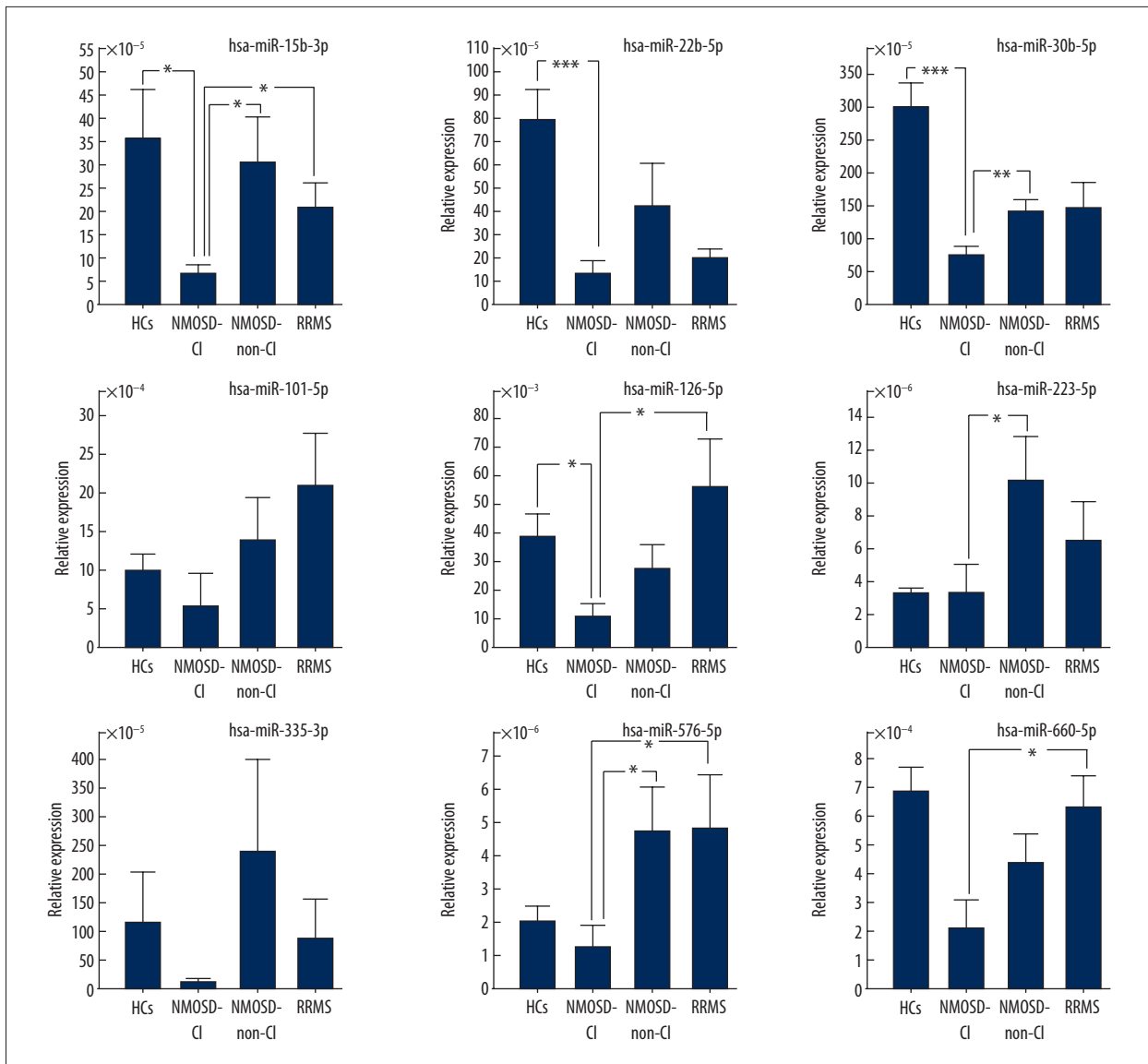


**Figure 2.** The expression level of the 9 miRNAs in NMOSD-IC and NMOSD-non-IC, RRMS and HCs. NMOSD-IC – NMOSD patients with intracranial lesions; NMOSD-non-IC – NMOSD patients without intracranial lesions. RRMS – relapsing-remitting multiple sclerosis; HCs – healthy controls. The bar diagram shows the mean  $\Delta$ -ACT values and standard deviations. \*  $P < 0.05$ , \*\*  $P < 0.01$ , \*\*\*  $P < 0.001$ .

was no significant difference in the level of any of the 9 miRNAs between NMOSD-non-IC subgroup with RRMS, CIS and HCs. These results collectively suggested that it was the intracranial lesions in the NMOSD that correlate with the peripheral down-regulated miRNAs.

**The utility of miRNAs in diagnosis and differentiation of NMOSD and RRMS**

The correlation between miRNA levels with the development and clinical features of NMOSD and RRMS suggested that they could help in diagnosing and differentiating them. To test how

well these miRNAs discriminate individuals with demyelinating disease and controls and patients with different subtypes, we generated receiver operating characteristic (ROC) curves by plotting the sensitivity of the levels of these miRNAs against 1-specificity and calculating the area under the ROC curves (C statistic) for each population. As shown in Figure 3, the AUCs of miR-101-5p and miR-126-5p for discriminating NMOSD and control were 0.74 and 0.72(A), the AUCs of miR-101-5p, miR-126-5p and miR-660-5p for discriminating NMOSD from RRMS were 0.71, 0.72 and 0.69 respectively(B). When we combined these 3 miRNAs, the AUC was 0.72, 0.69, 0.71 and 0.72 in discriminating these 2 subtypes (C). We also calculated the

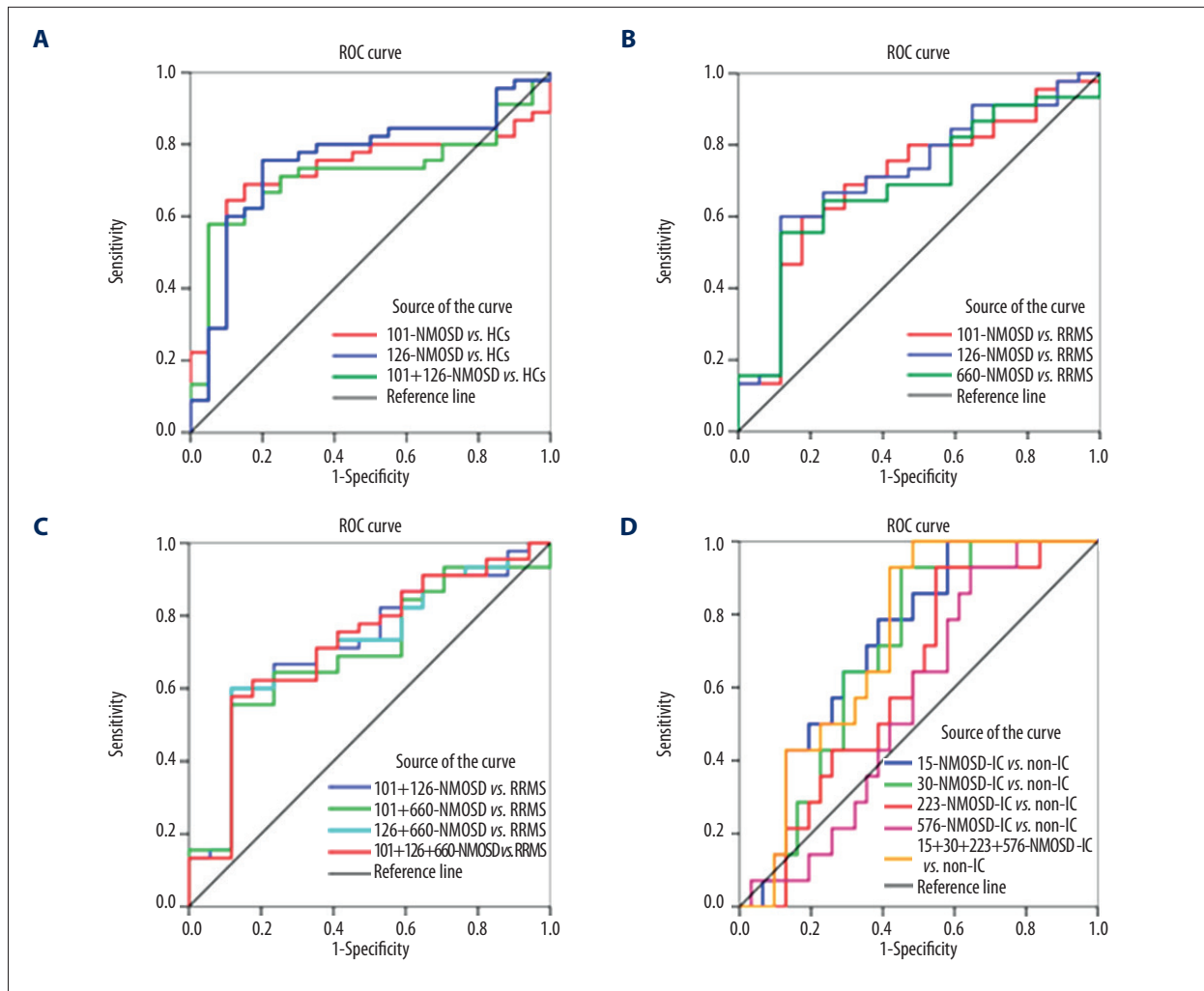


**Figure 3.** Discriminating power of miRNAs alone or in combination in differentiating NMOSD, RRMS from healthy controls and between subtypes (A-C), as well as differentiating intracranial lesions in NMOSD (D). Receiver operating characteristic curves (ROCs) were generated by plotting the sensitivity of the levels of these miRNAs against 1-specificity and calculating the area under the ROC curves (C statistic) for each population.

AUC of ROC for miR-15-5p, miR-30-5p, miR-223-5p and miR-576-5p, alone and in combination, in discriminating NMOSD-IC and NMOSD-non-IC. It turned out that all the AUCs were <0.8 (D). Combined, the results showed that none of the miRNA has enough power in the diagnosis and differential diagnosis of RRMS or NMOSD.

### Enrichment of miRNAs in molecular pathways

For the 5 miRNAs differentially expressed in NMOSD patients as compared to controls or RRMS, we found the most enrichment of miRNAs in pathways in cancer (4 of 5 ranked on position 1). Moreover, the neurotrophin signaling pathway, though not ranked before many pathways, was shared by all the 5 miRNAs (Supplementary Table 1)

### Discussion

NMOSD miRNA profiling was studied by next-generation sequencing (NGS), and the whole blood is thought to be an appropriate biospecimen for identification with neuroinflammatory diseases [16]. Previous research showed that a part of the miRNAs we selected are associated with inflammatory disease (miR-15b-5p and miR-30b-5p), others are associated with autoimmune disease (miR-22-5p, miR-101-5p, miR-223-5p and miR-660-5p). MiRWalk database showed that all the 9 miRNAs were specifically enriched in neurotrophin signaling pathway. Signaling activated by neurotrophins leads to a series of neuronal functions, such as axonal growth, cell survival, differentiation, dendritic arborization, synapse formation, plasticity and axonal guidance [21,22].

We found that some miRNAs (miR-22-5p, miR-30b-5p and miR-126-5p) were down-regulated in NMOSD, while others (miR-101-5p and miR-126-5p) were up-regulated in RRMS. Moreover, miR-223-5p and miR-576b-5p are associated with the certain clinical features in NMOSD, including the relapse and extent of visual impairment. MiR-30b-5p participates in restoration of injured optic nerve by regulating *sema3A* [23]. However, we did not observe any different expression between the patients with relapse or visual impairment. Instead, we found that the miR-576b-5p and miR-223-5p levels were associated with severe visual damage. These results confirm that miRNAs are correlated with CNS inflammatory demyelinating diseases, yet different subtypes may have different miRNA profiles. Nonetheless, the numbers of the patients RRMS was too small and the results look preliminary.

A major strength of the study is the finding of a strong reverse correlation between the peripheral miRNA expression levels with the intracranial (IC) lesions in NMOSD. In fact, the down-regulation of miRNAs (such as miR-22b-5p, miR-30b-5p and miR-126b-5p) revealed in NMOSD were confined to patients with intracranial lesions. In contrast, there was no significant difference in any of the 9 miRNAs between NMOSD patients without intracranial lesions (NMOSD-non-IC), RRMS and HCs, suggesting that these miRNAs were only associated with the NMOSD- IC subgroup, but not all the NMOSD patients. These observations are contrasted with Keller's study, in which miR-30b-5p and miR-15b-5p were demonstrated as differentiation biomarkers for NMOSD and MS/CIS [20]. The explanations for such differences could be multifold, the most important of which could be the considerable variation of incidence of intracranial lesions in NMOSD across different ethnicities, ranging from 12.5 to 89% [24–29]. The low incidence of intracranial lesions in our study might be a second explanation, with 5 non-specific small lesions locating in subcortical white matter and less than 3mm excluded from counting according to the MRI definition in the guidelines [20]. However, we do not really understand the causes of NMOSD-IC. In MS patients, Th17/Th1  $\geq 1$  relates to more lesions in brain than in spinal cord. Since NMOSD has more prominent imbalance of Th17/Th1 ratio than RRMS in the peripheral blood [30], the intracranial lesion-specific miRNAs could be also involved in the regulation of Th17 polarization, which, in turn, may increase the permeability and destruction of BBB through ICAM, VCAM, MMP-9 [31–33]. Studies have demonstrated the important roles of miR-30b-5p in regulation of humoral immune response as an inflammatory related factor [4], and bioinformatics analysis has also shown its acting on the IL-17 pathway. So, we consider that the cause of NMOSD-IC is the same as that of MS.

The functional significance of these NMOSD-associated miRNAs is not clear. It is interesting to find that these miRNAs were dominantly enriched in the cancer pathways and neurotrophin signaling pathway. Although there is no functional study confirming the involvement of cancer signaling pathway in inflammatory demyelinating diseases, there have been several studies confirming the role of neurotrophin factors, e.g. ciliary neurotrophic factor (CNTF) and p75NTR neurotrophin receptor, in multiple sclerosis [21,22]. Thus, it is intriguing to further investigate what neurotrophin factor genes are targeted by these miRNAs and what mechanisms by which are involved in NMOSD. The difference of miRNA levels in whole blood between patients and controls suggest that they may be candidate diagnostic and differential biomarkers for these disease entities. However, the discriminating power of any of the miRNAs alone or in combination were not strong enough (all AUCs of ROC were less than 0.8) to ensure diagnosis and differentiation of NMOSD or RRMS. Nor was the discrimination ensured by any miRNA alone or in combination between NMOSD patients with intracranial lesions from those without at the diagnostic level.

## Conclusions

In summary, in a verification study, we confirmed that certain miRNAs in the whole blood are associated with NMOSD and RRMS with distinct profiles. We also demonstrated that miRNAs are only reversely correlated to the intracranial lesions in NMOSD. However, contrasting to Keller's study, none of the miRNA alone or in combination was powerful to ensure the diagnosis and differentiation of these disease subtypes. Future studies with expanded sample size (especially that of RRMS and CIS patients) and functional studies are needed to verify our findings.

## Acknowledgments

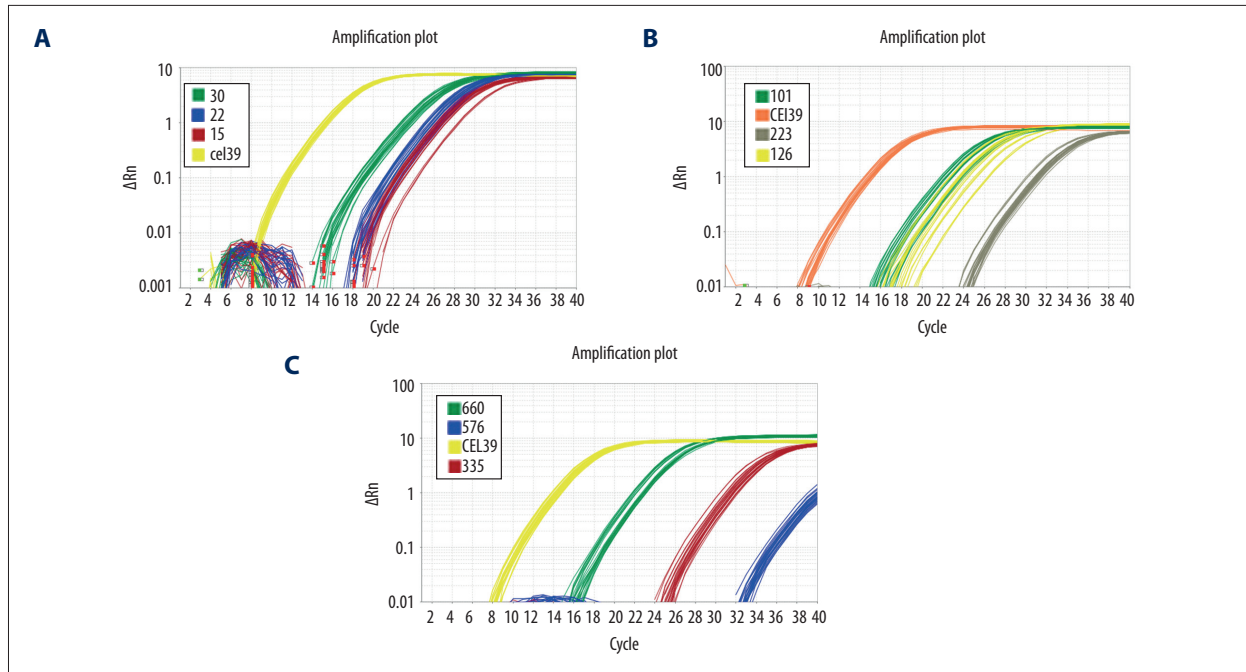
We thank the blood donors, The Core lab staffs of the First Affiliated Hospital of Fujian Medical University Hospital, and our colleagues especially the NMO research team for their helpful participation and comments.

## Conflict of interest

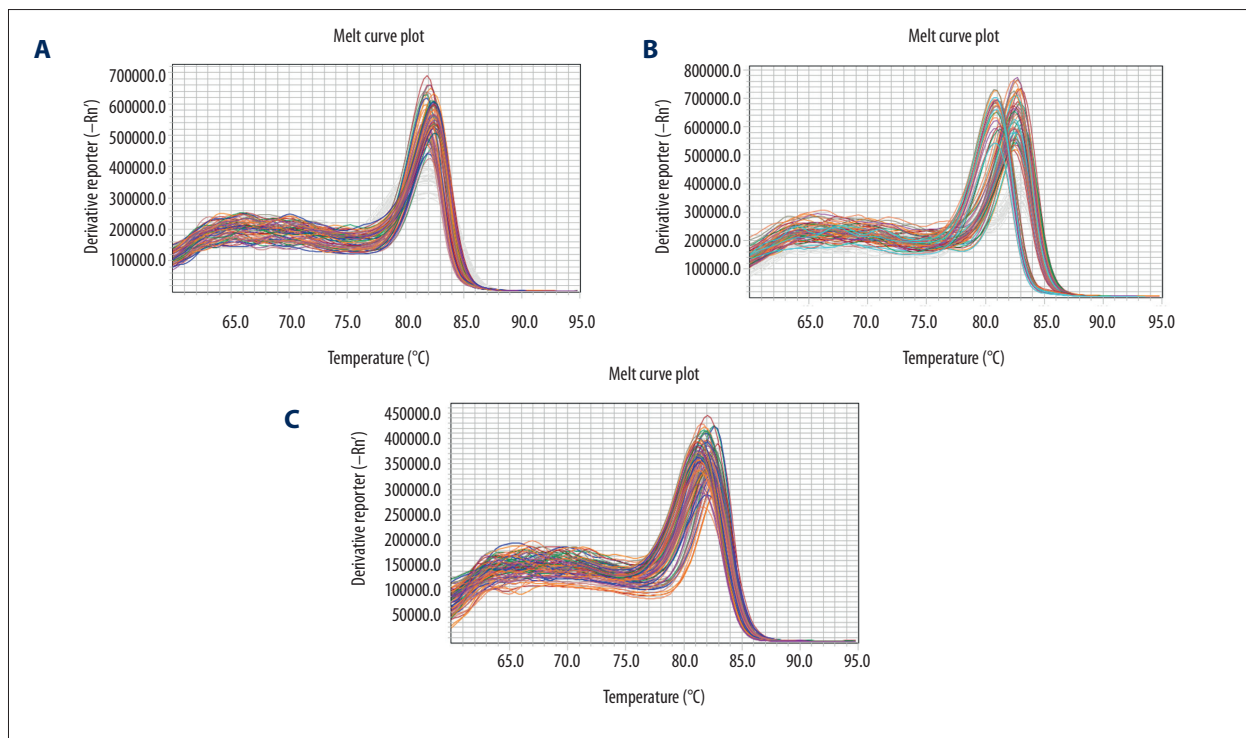
The authors declare that they have no conflict of interest.



## Supplementary Files



**Supplementary Figure 1.** Amplification plot of the miRNAs. A is the amplification curves of miR-15b-3p, miR-22b-5p, miR-30b-5p and cel39, B is the amplification curves of miR-101-5p, miR-126-5p, miR-223-5p and cel39, C is the amplification curves of miR-335-3p, miR-576-5p, miR-660-5p and cel39.



**Supplementary Figure 2.** Melting curves of the miRNAs. A is the melt curves of miR-15b-3p, miR-22b-5p, miR-30b-5p and cel39, B is the melt curves of miR-101-5p, miR-126-5p, miR-223-5p and cel39, C is the melt curves of miR-335-3p, miR-576-5p, miR-660-5p and cel39.

**Supplementary Table 1.** Enrichment of NMOSD-associated miRNAs in the molecular pathways.

MI RNA	PathName	PathFg	PathBg	GenomeFG	GenomeBG	P value	BH
hsa-miR-101-5p	Insulin signaling pathway	87	139	8485	19747	2.34E-06	0.00045371
hsa-miR-101-5p	Endocytosis	109	187	8485	19747	1.65E-05	0.003114265
hsa-miR-101-5p	Long term potentiation	48	71	8485	19747	2.36E-05	0.004468536
hsa-miR-101-5p	Colorectal cancer	56	86	8485	19747	2.78E-05	0.005217761
hsa-miR-101-5p	Neurotrophin signaling pathway	78	129	8485	19747	4.52E-05	0.008402147
hsa-miR-101-5p	Glioma	44	65	8485	19747	4.89E-05	0.009095575
hsa-miR-101-5p	Adherens junction	50	76	8485	19747	4.92E-05	0.009146105
hsa-miR-101-5p	Pathways in cancer	176	330	8485	19747	8.55E-05	0.015646108
hsa-miR-101-5p	Endometrial cancer	36	52	8485	19747	0.000115328	0.020759015
hsa-miR-101-5p	Wnt signaling pathway	88	152	8485	19747	0.000143178	0.025628775
hsa-miR-101-5p	Axon guidance	76	129	8485	19747	0.000185502	0.032833892
hsa-miR-101-5p	T cell receptor signaling pathway	66	110	8485	19747	0.000231552	0.040753187
hsa-miR-101-5p	ErbB signaling pathway	55	89	8485	19747	0.000260331	0.045557925
hsa-miR-101-5p	Chronic myeloid leukemia	47	75	8485	19747	0.000452969	0.077910691
hsa-miR-101-5p	Phosphatidylinositol signaling system	47	76	8485	19747	0.000695386	0.117520317
hsa-miR-101-5p	Calcium signaling pathway	98	178	8485	19747	0.000741421	0.125300102
hsa-miR-101-5p	Chemokine signaling pathway	103	189	8485	19747	0.000887525	0.148216608
hsa-miR-101-5p	Ubiquitin mediated proteolysis	76	134	8485	19747	0.000905223	0.151172313
hsa-miR-101-5p	Melanoma	44	71	8485	19747	0.000956101	0.158712713
hsa-miR-101-5p	Renal cell carcinoma	44	71	8485	19747	0.000956101	0.158712713
hsa-miR-101-5p	Non small cell lung cancer	35	54	8485	19747	0.000981599	0.16294541
hsa-miR-101-5p	B cell receptor signaling pathway	46	75	8485	19747	0.001018064	0.167980536
hsa-miR-101-5p	Type II diabetes mellitus	32	49	8485	19747	0.001327476	0.215051074
hsa-miR-101-5p	mTOR signaling pathway	34	53	8485	19747	0.001507004	0.241366957
hsa-miR-101-5p	Gap junction	53	90	8485	19747	0.001672357	0.265904786
hsa-miR-101-5p	Prostate cancer	52	89	8485	19747	0.002335429	0.361991448
hsa-miR-101-5p	Fc gamma R mediated phagocytosis	56	97	8485	19747	0.00236227	0.366151908
hsa-miR-101-5p	Adipocytokine signaling pathway	42	70	8485	19747	0.00300524	0.453791189
hsa-miR-101-5p	MAPK signaling pathway	139	272	8485	19747	0.003964632	0.582800901
hsa-miR-101-5p	Pancreatic cancer	44	75	8485	19747	0.004398819	0.637828798
hsa-miR-101-5p	Focal adhesion	106	203	8485	19747	0.004776226	0.687776614
hsa-miR-101-5p	Purine metabolism	84	158	8485	19747	0.006105552	0.844734415
hsa-miR-101-5p	GnRH signaling pathway	58	105	8485	19747	0.00745423	0.994695317
hsa-miR-101-5p	Long term depression	40	73	8485	19747	0.027582947	1

MiRNA	PathName	PathFg	PathBg	GenomeFG	GenomeBG	P value	BH
hsa-miR-101-5p	Jak STAT signaling pathway	82	156	8485	19747	0.009686644	1
hsa-miR-101-5p	Small cell lung cancer	46	84	8485	19747	0.019339805	1
hsa-miR-101-5p	SNARE interactions in vesicular transport	23	39	8485	19747	0.032118483	1
hsa-miR-101-5p	Acute myeloid leukemia	34	58	8485	19747	0.011708417	1
hsa-miR-101-5p	Vascular smooth muscle contraction	59	116	8485	19747	0.052274252	1
hsa-miR-101-5p	Thyroid cancer	19	29	8485	19747	0.011984069	1
hsa-miR-101-5p	Lysine degradation	27	45	8485	19747	0.015826415	1
hsa-miR-101-5p	Epithelial cell signaling in Helicobacter pylori infection	38	71	8485	19747	0.047178139	1
hsa-miR-101-5p	Metabolic pathways	499	1091	8485	19747	0.030975475	1
hsa-miR-101-5p	VEGF signaling pathway	44	78	8485	19747	0.011418856	1
hsa-miR-101-5p	Fc epsilon RI signaling pathway	43	82	8485	19747	0.052777799	1
hsa-miR-101-5p	Amyotrophic lateral sclerosis ALS	30	55	8485	19747	0.055429268	1
hsa-miR-101-5p	Primary bile acid biosynthesis	11	16	8485	19747	0.033948998	1
hsa-miR-101-5p	Nicotinate and nicotinamide metabolism	16	24	8485	19747	0.01649091	1
hsa-miR-101-5p	Non homologous end joining	10	13	8485	19747	0.014005601	1
hsa-miR-101-5p	Inositol phosphate metabolism	32	54	8485	19747	0.01154892	1
hsa-miR-101-5p	Peroxisome	44	79	8485	19747	0.015200198	1
hsa-miR-101-5p	PPAR signaling pathway	39	70	8485	19747	0.021327693	1
hsa-miR-101-5p	Cell adhesion molecules CAMs	67	133	8485	19747	0.050655518	1
hsa-miR-101-5p	Nitrogen metabolism	16	23	8485	19747	0.009100855	1
hsa-miR-101-5p	Aldosterone regulated sodium reabsorption	24	42	8485	19747	0.045107589	1
hsa-miR-101-5p	O Glycan biosynthesis	20	30	8485	19747	0.007542929	1
hsa-miR-101-5p	Melanogenesis	54	102	8485	19747	0.026728523	1
hsa-miR-101-5p	Lysosome	62	121	8485	19747	0.040474391	1
hsa-miR-101-5p	Tight junction	68	132	8485	19747	0.029075318	1
hsa-miR-101-5p	Regulation of actin cytoskeleton	103	212	8485	19747	0.056232548	1
hsa-miR-101-5p	TGF beta signaling pathway	46	86	8485	19747	0.031594456	1
hsa-miR-126-5p	Pathways in cancer	176	330	8124	19747	4.43E-06	0.000855946
hsa-miR-126-5p	Small cell lung cancer	55	84	8124	19747	5.61E-06	0.001083654
hsa-miR-126-5p	Neurotrophin signaling pathway	76	129	8124	19747	3.35E-05	0.006370669
hsa-miR-126-5p	Colorectal cancer	54	86	8124	19747	4.05E-05	0.007697755
hsa-miR-126-5p	Chronic myeloid leukemia	48	75	8124	19747	5.29E-05	0.01004258
hsa-miR-126-5p	Apoptosis	53	87	8124	19747	0.000151403	0.027706725
hsa-miR-126-5p	Ubiquitin mediated proteolysis	76	134	8124	19747	0.000189394	0.034280231

MI RNA	PathName	PathFg	PathBg	GenomeFG	GenomeBG	P value	BH
hsa-miR-126-5p	Insulin signaling pathway	78	139	8124	19747	0.000249692	0.044445215
hsa-miR-126-5p	Pentose and glucuronate interconversions	21	28	8124	19747	0.000289367	0.051279554
hsa-miR-126-5p	ErbB signaling pathway	53	89	8124	19747	0.00034132	0.060413711
hsa-miR-126-5p	Non small cell lung cancer	35	54	8124	19747	0.000373669	0.065765685
hsa-miR-126-5p	MAPK signaling pathway	139	272	8124	19747	0.000528068	0.092411913
hsa-miR-126-5p	Glioma	40	65	8124	19747	0.000709157	0.123393247
hsa-miR-126-5p	Ascorbate and aldarate metabolism	19	26	8124	19747	0.000976366	0.168911356
hsa-miR-126-5p	p53 signaling pathway	41	68	8124	19747	0.001096874	0.189759278
hsa-miR-126-5p	Endocytosis	98	187	8124	19747	0.001158089	0.200349415
hsa-miR-126-5p	Type II diabetes mellitus	31	49	8124	19747	0.001447572	0.247534873
hsa-miR-126-5p	Prostate cancer	51	89	8124	19747	0.001488647	0.254558697
hsa-miR-126-5p	Pancreatic cancer	44	75	8124	19747	0.001614467	0.274459422
hsa-miR-126-5p	Renal cell carcinoma	42	71	8124	19747	0.001632088	0.277455025
hsa-miR-126-5p	T cell receptor signaling pathway	61	110	8124	19747	0.001662737	0.282665317
hsa-miR-126-5p	Axon guidance	70	129	8124	19747	0.001728524	0.293849129
hsa-miR-126-5p	Wnt signaling pathway	79	152	8124	19747	0.004369155	0.642265816
hsa-miR-126-5p	Melanoma	40	71	8124	19747	0.00685062	0.897431176
hsa-miR-126-5p	Focal adhesion	101	203	8124	19747	0.007764884	0.978375349
hsa-miR-126-5p	VEGF signaling pathway	41	78	8124	19747	0.027028017	1
hsa-miR-126-5p	ECM receptor interaction	43	84	8124	19747	0.039640345	1
hsa-miR-126-5p	GnRH signaling pathway	52	105	8124	19747	0.05015675	1
hsa-miR-126-5p	Progesterone mediated oocyte maturation	44	88	8124	19747	0.057399498	1
hsa-miR-126-5p	ABC transporters	26	44	8124	19747	0.012230769	1
hsa-miR-126-5p	Endometrial cancer	28	52	8124	19747	0.043389343	1
hsa-miR-126-5p	Non homologous end joining	9	13	8124	19747	0.038757914	1
hsa-miR-126-5p	Adipocytokine signaling pathway	39	70	8124	19747	0.009610695	1
hsa-miR-126-5p	B cell receptor signaling pathway	39	75	8124	19747	0.037002266	1
hsa-miR-126-5p	Primary immunodeficiency	20	35	8124	19747	0.040787619	1
hsa-miR-126-5p	Cell adhesion molecules CAMs	68	133	8124	19747	0.012382036	1
hsa-miR-126-5p	Cell cycle	64	124	8124	19747	0.011604645	1
hsa-miR-126-5p	Acute myeloid leukemia	31	58	8124	19747	0.038959432	1
hsa-miR-126-5p	Drug metabolism other enzymes	29	51	8124	19747	0.016791375	1
hsa-miR-126-5p	PPAR signaling pathway	36	70	8124	19747	0.052375031	1
hsa-miR-126-5p	Starch and sucrose metabolism	29	52	8124	19747	0.023271708	1
hsa-miR-126-5p	mTOR signaling pathway	29	53	8124	19747	0.03154144	1

MiRNA	PathName	PathFg	PathBg	GenomeFG	GenomeBG	P value	BH
hsa-miR-126-5p	Aldosterone regulated sodium reabsorption	25	42	8124	19747	0.012305735	1
hsa-miR-126-5p	Tight junction	64	132	8124	19747	0.052078934	1
hsa-miR-126-5p	Porphyrin and chlorophyll metabolism	25	41	8124	19747	0.008117058	1
hsa-miR-126-5p	Regulation of actin cytoskeleton	99	212	8124	19747	0.057272856	1
hsa-miR-126-5p	Protein export	14	23	8124	19747	0.044570896	1
hsa-miR-22-5p	Pathways in cancer	257	330	11812	19747	1.83E-12	3.56E-10
hsa-miR-22-5p	Axon guidance	110	129	11812	19747	2.59E-10	5.00E-08
hsa-miR-22-5p	Endocytosis	149	187	11812	19747	4.95E-09	9.40E-07
hsa-miR-22-5p	Wnt signaling pathway	124	152	11812	19747	6.55E-09	1.24E-06
hsa-miR-22-5p	MAPK signaling pathway	207	272	11812	19747	8.91E-09	1.69E-06
hsa-miR-22-5p	Colorectal cancer	75	86	11812	19747	2.35E-08	4.45E-06
hsa-miR-22-5p	Cell adhesion molecules CAMs	108	133	11812	19747	9.92E-08	1.85E-05
hsa-miR-22-5p	ErbB signaling pathway	76	89	11812	19747	1.37E-07	2.56E-05
hsa-miR-22-5p	Neurotrophin signaling pathway	103	129	11812	19747	9.50E-07	0.000173927
hsa-miR-22-5p	Focal adhesion	154	203	11812	19747	9.68E-07	0.000177219
hsa-miR-22-5p	Chronic myeloid leukemia	64	75	11812	19747	1.43E-06	0.000260548
hsa-miR-22-5p	Small cell lung cancer	70	84	11812	19747	2.90E-06	0.000522275
hsa-miR-22-5p	Glioma	56	65	11812	19747	3.48E-06	0.000622806
hsa-miR-22-5p	Type II diabetes mellitus	44	49	11812	19747	3.52E-06	0.000629532
hsa-miR-22-5p	B cell receptor signaling pathway	63	75	11812	19747	5.33E-06	0.000948843
hsa-miR-22-5p	Prostate cancer	73	89	11812	19747	5.80E-06	0.00102714
hsa-miR-22-5p	T cell receptor signaling pathway	87	110	11812	19747	1.34E-05	0.002351804
hsa-miR-22-5p	Leukocyte transendothelial migration	91	116	11812	19747	1.57E-05	0.002744659
hsa-miR-22-5p	Regulation of actin cytoskeleton	156	212	11812	19747	1.73E-05	0.003024113
hsa-miR-22-5p	Apoptosis	70	87	11812	19747	3.23E-05	0.005550083
hsa-miR-22-5p	Adherens junction	62	76	11812	19747	4.08E-05	0.006975744
hsa-miR-22-5p	Pancreatic cancer	61	75	11812	19747	5.61E-05	0.009538741
hsa-miR-22-5p	Fc gamma R mediated phagocytosis	76	97	11812	19747	8.38E-05	0.014085998
hsa-miR-22-5p	Endometrial cancer	44	52	11812	19747	0.000101849	0.017008724
hsa-miR-22-5p	Ubiquitin mediated proteolysis	101	134	11812	19747	0.000107433	0.017941347
hsa-miR-22-5p	Insulin signaling pathway	104	139	11812	19747	0.00014148	0.023485705
hsa-miR-22-5p	Non small cell lung cancer	45	54	11812	19747	0.000179093	0.029550271
hsa-miR-22-5p	Melanogenesis	78	102	11812	19747	0.000288309	0.047282657
hsa-miR-22-5p	VEGF signaling pathway	61	78	11812	19747	0.000454736	0.073212496
hsa-miR-22-5p	Acute myeloid leukemia	47	58	11812	19747	0.000474205	0.076346974

MiRNA	PathName	PathFg	PathBg	GenomeFG	GenomeBG	P value	BH
hsa-miR-22-5p	p53 signaling pathway	54	68	11812	19747	0.000481292	0.077197402
hsa-miR-22-5p	Dorso ventral axis formation	22	24	11812	19747	0.000620089	0.098594229
hsa-miR-22-5p	Melanoma	55	71	11812	19747	0.001297563	0.197229622
hsa-miR-22-5p	Calcium signaling pathway	125	178	11812	19747	0.002461358	0.356896943
hsa-miR-22-5p	Long term potentiation	54	71	11812	19747	0.002984255	0.426748527
hsa-miR-22-5p	Renal cell carcinoma	54	71	11812	19747	0.002984255	0.426748527
hsa-miR-22-5p	Aldosterone regulated sodium reabsorption	34	42	11812	19747	0.003015903	0.431274084
hsa-miR-22-5p	Basal cell carcinoma	43	55	11812	19747	0.003152907	0.447712777
hsa-miR-22-5p	Amyotrophic lateral sclerosis ALS	43	55	11812	19747	0.003152907	0.447712777
hsa-miR-22-5p	Lysine degradation	36	45	11812	19747	0.003356409	0.476610046
hsa-miR-22-5p	Adipocytokine signaling pathway	53	70	11812	19747	0.003848062	0.542576696
hsa-miR-22-5p	mTOR signaling pathway	41	53	11812	19747	0.005514037	0.733366983
hsa-miR-22-5p	Epithelial cell signaling in Helicobacter pylori infection	53	71	11812	19747	0.006391491	0.824502359
hsa-miR-22-5p	Hypertrophic cardiomyopathy HCM	63	86	11812	19747	0.006423679	0.828654588
hsa-miR-22-5p	Arrhythmogenic right ventricular cardiomyopathy ARVC	55	74	11812	19747	0.006436624	0.830010217
hsa-miR-22-5p	Chondroitin sulfate biosynthesis	19	22	11812	19747	0.007196724	0.899590471
hsa-miR-22-5p	Phosphatidylinositol signaling system	56	76	11812	19747	0.0081223	0.966553692
hsa-miR-22-5p	Prion diseases	28	35	11812	19747	0.009551427	1
hsa-miR-22-5p	Heparan sulfate biosynthesis	21	26	11812	19747	0.020411929	1
hsa-miR-22-5p	Fc epsilon RI signaling pathway	58	82	11812	19747	0.026603879	1
hsa-miR-22-5p	GnRH signaling pathway	73	105	11812	19747	0.025144507	1
hsa-miR-22-5p	Chemokine signaling pathway	128	189	11812	19747	0.014802878	1
hsa-miR-22-5p	N Glycan biosynthesis	35	46	11812	19747	0.01561363	1
hsa-miR-22-5p	TGF beta signaling pathway	62	86	11812	19747	0.0120408	1
hsa-miR-22-5p	Hedgehog signaling pathway	40	56	11812	19747	0.048585074	1
hsa-miR-22-5p	ABC transporters	33	44	11812	19747	0.026093417	1
hsa-miR-22-5p	Type I diabetes mellitus	32	44	11812	19747	0.05300307	1
hsa-miR-22-5p	Bladder cancer	33	43	11812	19747	0.015183097	1
hsa-miR-22-5p	Jak STAT signaling pathway	108	156	11812	19747	0.009237744	1
hsa-miR-22-5p	Valine leucine and isoleucine degradation	33	45	11812	19747	0.04218212	1
hsa-miR-22-5p	Long term depression	51	73	11812	19747	0.049326477	1
hsa-miR-22-5p	SNARE interactions in vesicular transport	30	39	11812	19747	0.019292832	1
hsa-miR-22-5p	Caffeine metabolism	7	7	11812	19747	0.027380781	1
hsa-miR-22-5p	Dilated cardiomyopathy	67	94	11812	19747	0.013884057	1

MI RNA	PathName	PathFg	PathBg	GenomeFG	GenomeBG	P value	BH
hsa-miR-22-5p	Progesterone mediated oocyte maturation	61	88	11812	19747	0.04174596	1
hsa-miR-30b-5p	Pathways in cancer	156	330	6411	19747	1.23E-08	2.38E-06
hsa-miR-30b-5p	Adherens junction	46	76	6411	19747	4.52E-07	8.67E-05
hsa-miR-30b-5p	Colorectal cancer	49	86	6411	19747	2.38E-06	0.000450104
hsa-miR-30b-5p	ErbB signaling pathway	50	89	6411	19747	3.30E-06	0.000623737
hsa-miR-30b-5p	Glioma	39	65	6411	19747	4.53E-06	0.000851658
hsa-miR-30b-5p	Ubiquitin mediated proteolysis	68	134	6411	19747	8.38E-06	0.001567818
hsa-miR-30b-5p	Non small cell lung cancer	33	54	6411	19747	1.41E-05	0.002637103
hsa-miR-30b-5p	Wnt signaling pathway	73	152	6411	19747	4.52E-05	0.008184389
hsa-miR-30b-5p	Pancreatic cancer	41	75	6411	19747	5.81E-05	0.010463047
hsa-miR-30b-5p	Chronic myeloid leukemia	41	75	6411	19747	5.81E-05	0.010463047
hsa-miR-30b-5p	Axon guidance	63	129	6411	19747	7.86E-05	0.013994427
hsa-miR-30b-5p	Phosphatidylinositol signaling system	41	76	6411	19747	8.68E-05	0.015459153
hsa-miR-30b-5p	Apoptosis	45	87	6411	19747	0.000151014	0.026578382
hsa-miR-30b-5p	MAPK signaling pathway	117	272	6411	19747	0.000158251	0.02785209
hsa-miR-30b-5p	Long term potentiation	38	71	6411	19747	0.000193569	0.034068087
hsa-miR-30b-5p	Melanoma	38	71	6411	19747	0.000193569	0.034068087
hsa-miR-30b-5p	Endocytosis	84	187	6411	19747	0.000238243	0.041930686
hsa-miR-30b-5p	Prostate cancer	45	89	6411	19747	0.000295855	0.052070558
hsa-miR-30b-5p	Neurotrophin signaling pathway	60	129	6411	19747	0.000594457	0.099868714
hsa-miR-30b-5p	Long term depression	37	73	6411	19747	0.00092949	0.150577329
hsa-miR-30b-5p	Amyotrophic lateral sclerosis ALS	29	55	6411	19747	0.001463924	0.229836089
hsa-miR-30b-5p	Regulation of actin cytoskeleton	89	212	6411	19747	0.00218848	0.334837477
hsa-miR-30b-5p	Renal cell carcinoma	35	71	6411	19747	0.00233667	0.357510548
hsa-miR-30b-5p	Melanogenesis	47	102	6411	19747	0.002785731	0.42343105
hsa-miR-30b-5p	Endometrial cancer	27	52	6411	19747	0.002814214	0.424946331
hsa-miR-30b-5p	Focal adhesion	85	203	6411	19747	0.002953579	0.44599037
hsa-miR-30b-5p	Gap junction	42	90	6411	19747	0.003411486	0.511722866
hsa-miR-30b-5p	Progesterone mediated oocyte maturation	41	88	6411	19747	0.003926434	0.585346476
hsa-miR-30b-5p	Acute myeloid leukemia	29	58	6411	19747	0.004116963	0.613427489
hsa-miR-30b-5p	Protein export	14	23	6411	19747	0.004720087	0.703292942
hsa-miR-30b-5p	O Glycan biosynthesis	17	30	6411	19747	0.005327257	0.788434095
hsa-miR-30b-5p	Arrhythmogenic right ventricular cardiomyopathy ARVC	35	74	6411	19747	0.005487362	0.806642248
hsa-miR-30b-5p	Inositol phosphate metabolism	27	54	6411	19747	0.005531749	0.813167132

MiRNA	PathName	PathFg	PathBg	GenomeFG	GenomeBG	P value	BH
hsa-miR-30b-5p	Aldosterone regulated sodium reabsorption	22	42	6411	19747	0.005864446	0.862073569
hsa-miR-30b-5p	mTOR signaling pathway	26	53	6411	19747	0.008761618	1
hsa-miR-30b-5p	Ascorbate and aldarate metabolism	14	26	6411	19747	0.019511549	1
hsa-miR-30b-5p	Type II diabetes mellitus	24	49	6411	19747	0.011815574	1
hsa-miR-30b-5p	p53 signaling pathway	30	68	6411	19747	0.029133167	1
hsa-miR-30b-5p	Small cell lung cancer	38	84	6411	19747	0.009658053	1
hsa-miR-30b-5p	T cell receptor signaling pathway	47	110	6411	19747	0.015157895	1
hsa-miR-30b-5p	Leukocyte transendothelial migration	49	116	6411	19747	0.016941064	1
hsa-miR-30b-5p	Cell adhesion molecules CAMs	53	133	6411	19747	0.043304347	1
hsa-miR-30b-5p	Vascular smooth muscle contraction	50	116	6411	19747	0.010372332	1
hsa-miR-30b-5p	Thyroid cancer	16	29	6411	19747	0.009556352	1
hsa-miR-30b-5p	Insulin signaling pathway	59	139	6411	19747	0.008447402	1
hsa-miR-30b-5p	ABC transporters	20	44	6411	19747	0.048992968	1
hsa-miR-30b-5p	TGF beta signaling pathway	39	86	6411	19747	0.008411963	1
hsa-miR-30b-5p	Tight junction	55	132	6411	19747	0.016223801	1
hsa-miR-30b-5p	Hypertrophic cardiomyopathy HCM	36	86	6411	19747	0.042112097	1
hsa-miR-30b-5p	Bladder cancer	20	43	6411	19747	0.03804409	1
hsa-miR-30b-5p	Fc gamma R mediated phagocytosis	42	97	6411	19747	0.016262241	1
hsa-miR-30b-5p	Dilated cardiomyopathy	39	94	6411	19747	0.040911576	1
hsa-miR-30b-5p	Calcium signaling pathway	73	178	6411	19747	0.00990428	1
hsa-miR-30b-5p	Fc epsilon RI signaling pathway	37	82	6411	19747	0.011088588	1
hsa-miR-660-5p	Chronic myeloid leukemia	47	75	5834	19747	2.75E-09	5.30E-07
hsa-miR-660-5p	Pathways in cancer	145	330	5834	19747	1.63E-08	3.12E-06
hsa-miR-660-5p	Glioma	41	65	5834	19747	2.14E-08	4.08E-06
hsa-miR-660-5p	Insulin signaling pathway	71	139	5834	19747	7.71E-08	1.46E-05
hsa-miR-660-5p	Apoptosis	49	87	5834	19747	1.69E-07	3.19E-05
hsa-miR-660-5p	MAPK signaling pathway	119	272	5834	19747	4.01E-07	7.50E-05
hsa-miR-660-5p	ErbB signaling pathway	49	89	5834	19747	4.34E-07	8.11E-05
hsa-miR-660-5p	Non small cell lung cancer	33	54	5834	19747	1.44E-06	0.000268502
hsa-miR-660-5p	Pancreatic cancer	41	75	5834	19747	4.73E-06	0.000864782
hsa-miR-660-5p	Renal cell carcinoma	39	71	5834	19747	6.86E-06	0.001248947
hsa-miR-660-5p	Wnt signaling pathway	70	152	5834	19747	1.17E-05	0.002111246
hsa-miR-660-5p	Adipocytokine signaling pathway	38	70	5834	19747	1.30E-05	0.002331179
hsa-miR-660-5p	Small cell lung cancer	43	84	5834	19747	2.51E-05	0.004445646
hsa-miR-660-5p	Neurotrophin signaling pathway	60	129	5834	19747	3.33E-05	0.005852361



MI RNA	PathName	PathFg	PathBg	GenomeFG	GenomeBG	P value	BH
hsa-miR-660-5p	Aldosterone regulated sodium reabsorption	25	42	5834	19747	5.11E-05	0.008849739
hsa-miR-660-5p	Prostate cancer	44	89	5834	19747	6.07E-05	0.010434751
hsa-miR-660-5p	Calcium signaling pathway	77	178	5834	19747	6.61E-05	0.011367391
hsa-miR-660-5p	Axon guidance	59	129	5834	19747	7.01E-05	0.012062999
hsa-miR-660-5p	Vascular smooth muscle contraction	54	116	5834	19747	7.81E-05	0.01334723
hsa-miR-660-5p	VEGF signaling pathway	39	78	5834	19747	0.000114223	0.019189454
hsa-miR-660-5p	Dilated cardiomyopathy	45	94	5834	19747	0.000133217	0.022247276
hsa-miR-660-5p	Hypertrophic cardiomyopathy HCM	41	86	5834	19747	0.000290082	0.046703244
hsa-miR-660-5p	Ether lipid metabolism	21	36	5834	19747	0.000300946	0.048452314
hsa-miR-660-5p	Adherens junction	37	76	5834	19747	0.000335452	0.053672279
hsa-miR-660-5p	Long term potentiation	35	71	5834	19747	0.000356024	0.056963838
hsa-miR-660-5p	Melanoma	35	71	5834	19747	0.000356024	0.056963838
hsa-miR-660-5p	Type II diabetes mellitus	26	49	5834	19747	0.000474592	0.075460141
hsa-miR-660-5p	T cell receptor signaling pathway	49	110	5834	19747	0.000588087	0.092917806
hsa-miR-660-5p	Colorectal cancer	40	86	5834	19747	0.000640805	0.10124723
hsa-miR-660-5p	Heparan sulfate biosynthesis	16	26	5834	19747	0.000700414	0.110665477
hsa-miR-660-5p	Phosphatidylinositol signaling system	36	76	5834	19747	0.00077014	0.12091191
hsa-miR-660-5p	Fc epsilon RI signaling pathway	38	82	5834	19747	0.000942721	0.148007141
hsa-miR-660-5p	Chondroitin sulfate biosynthesis	14	22	5834	19747	0.000946761	0.148641411
hsa-miR-660-5p	B cell receptor signaling pathway	35	75	5834	19747	0.001262727	0.195722739
hsa-miR-660-5p	GnRH signaling pathway	46	105	5834	19747	0.001305999	0.202429883
hsa-miR-660-5p	Glycerophospholipid metabolism	33	70	5834	19747	0.001386882	0.214966783
hsa-miR-660-5p	Endometrial cancer	26	52	5834	19747	0.001513571	0.23460344
hsa-miR-660-5p	alpha Linolenic acid metabolism	12	19	5834	19747	0.002432594	0.36245658
hsa-miR-660-5p	Acute myeloid leukemia	27	58	5834	19747	0.004528781	0.638558156
hsa-miR-660-5p	Ubiquitin mediated proteolysis	54	134	5834	19747	0.004925757	0.689605994
hsa-miR-660-5p	Tight junction	53	132	5834	19747	0.005783875	0.798174774
hsa-miR-660-5p	Regulation of actin cytoskeleton	80	212	5834	19747	0.006113676	0.84368735
hsa-miR-660-5p	mTOR signaling pathway	24	53	5834	19747	0.010883105	1
hsa-miR-660-5p	Oocyte meiosis	43	112	5834	19747	0.027327133	1
hsa-miR-660-5p	Cell adhesion molecules CAMs	52	133	5834	19747	0.011277543	1
hsa-miR-660-5p	Glycerolipid metabolism	19	46	5834	19747	0.059110806	1
hsa-miR-660-5p	Keratan sulfate biosynthesis	8	15	5834	19747	0.045846187	1
hsa-miR-660-5p	Gap junction	35	90	5834	19747	0.035823644	1
hsa-miR-660-5p	Chemokine signaling pathway	67	189	5834	19747	0.045513457	1

MiRNA	PathName	PathFg	PathBg	GenomeFG	GenomeBG	P value	BH
hsa-miR-660-5p	Melanogenesis	40	102	5834	19747	0.022771607	1
hsa-miR-660-5p	TGF beta signaling pathway	34	86	5834	19747	0.029933866	1
hsa-miR-660-5p	Endocytosis	68	187	5834	19747	0.025812976	1
hsa-miR-660-5p	Toll like receptor signaling pathway	39	105	5834	19747	0.05651642	1
hsa-miR-660-5p	Thyroid cancer	13	29	5834	19747	0.058252127	1
hsa-miR-660-5p	Fc gamma R mediated phagocytosis	39	97	5834	19747	0.015811658	1
hsa-miR-660-5p	SNARE interactions in vesicular transport	18	39	5834	19747	0.020642828	1
hsa-miR-660-5p	Long term depression	31	73	5834	19747	0.012611827	1
hsa-miR-660-5p	Progesterone mediated oocyte maturation	35	88	5834	19747	0.025436504	1
hsa-miR-660-5p	Inositol phosphate metabolism	22	54	5834	19747	0.051713668	1
hsa-miR-660-5p	p53 signaling pathway	28	68	5834	19747	0.026708436	1
hsa-miR-660-5p	Arrhythmogenic right ventricular cardiomyopathy ARVC	30	74	5834	19747	0.028017892	1
hsa-miR-660-5p	Focal adhesion	76	203	5834	19747	0.009166013	1
hsa-miR-660-5p	Jak STAT signaling pathway	58	156	5834	19747	0.023864483	1
hsa-miR-660-5p	Valine leucine and isoleucine degradation	19	45	5834	19747	0.047463292	1

References:

- Keller A, Leidinger P, Bauer A et al: Toward the blood-borne miRNome of human diseases. *Nat Methods*, 2011; 8(10): 841-43
- Finnerty JR, Wang WX, Hébert SS et al: The miR-15/107 group of microRNA genes: Evolutionary biology, cellular functions, and roles in human diseases. *J Mol Biol*, 2010; 402(3): 491-509
- Maciejak A, Kiliszek M, Opolski G et al: MiR-22-5p revealed as a potential biomarker involved in the acute phase of myocardial infarction via profiling of circulating microRNAs. *Mol Med Rep*, 2016; 14(3): 2867-75
- Duan ZQ, Shi JD, Wu MN et al: Influence of miR-30b regulating humoral immune response by genetic difference. *Immunol Res*, 2016; 64(1): 181-90
- Fernández-Hernando C, Suárez Y, Rayner KJ et al: MicroRNAs in lipid metabolism. *Curr Opin Lipidol*, 2011; 22(2): 86-92
- Liu P, Ye F, Xie X et al: mir-101-3p is a key regulator of tumor metabolism in triple negative breast cancer targeting AMPK. *Oncotarget*, 2016; 7(23): 35188-98
- Qin D, Wang X, Li Y et al: MicroRNA-223-5p and -3p cooperatively suppress necroptosis in ischemic/reperfused hearts. *J Biol Chem*, 2016; 291(38): 20247-59
- Schober A, Nazari-Jahantigh M, Wei Y et al: MicroRNA-126-5p promotes endothelial proliferation and limits atherosclerosis by suppressing Dlk1. *Nat Med*, 2014; 20(4): 368-76
- Krishnan P, Ghosh S, Wang B et al: Next generation sequencing profiling identifies miR-574-3p and miR-660-5p as potential novel prognostic markers for breast cancer. *BMC Genomics*, 2015; 16: 735-51
- Mairinger FD, Ting S, Werner R et al: Different micro-RNA expression profiles distinguish subtypes of neuroendocrine tumors of the lung: Results of a profiling study. *Mod Pathol*, 2014; 27(12): 1632-40
- Siegel SR, Mackenzie J, Chaplin G et al: Circulating microRNAs involved in multiple sclerosis. *Mol Biol Rep*, 2012; 39(5): 6219-25
- Martinelli-Boneschi F, Fenoglio C, Brambilla P et al: MicroRNA and mRNA expression profile screening in multiple sclerosis patients to unravel novel pathogenic steps and identify potential biomarkers. *Neurosci Lett*, 2012; 508(1): 4-8
- Søndergaard HB, Hesse D, Krakauer M et al: Differential microRNA expression in blood in multiple sclerosis. *Mult Scler*, 2013; 19(14): 1849-57
- Keller A, Leidinger P, Steinmeyer F et al: Comprehensive analysis of microRNA profiles in multiple sclerosis including next-generation sequencing. *Mult Scler*, 2014; 20(3): 295-303
- Gandhi R, Healy B, Gholipour T et al: Circulating microRNAs as biomarkers for disease staging in multiple sclerosis. *Ann Neurol*, 2013; 73(6): 729-40
- Huang D, Wu W et al: Guidelines for the diagnosis and treatment of optic neuropathy spectrum disorders in China. *Chin J Neuroimmunol and Neurol*, 2016; 23(3): 155-66
- Wingerchuk DM, Banwell B, Bennett JL et al: International consensus diagnostic criteria for neuromyelitis optica spectrum disorders. *Neurology*, 2015; 85(2): 177-89
- Polman CH, Reingold SC, Banwell B et al: Diagnostic criteria for multiple sclerosis: 2010 revisions to the McDonald criteria. *Ann Neurol*, 2011; 69(2): 292-302
- Filippi M, Rocca MA, Ciccarelli O et al: MRI criteria for the diagnosis of multiple sclerosis: MAGNIMS consensus guidelines. *Lancet Neurol*, 2016; 15(3): 292-303
- Keller A, Leidinger P, Steinmeyer F et al: Comprehensive analysis of microRNA profiles in multiple sclerosis including next-generation sequencing. *Mult Scler*, 2014; 20(3): 295-303
- Keller A, Leidinger P, Meese E et al: Next-generation sequencing identifies altered whole blood microRNAs in neuromyelitis optica spectrum disorder which may permit discrimination from multiple sclerosis. *J Neuroinflammation*, 2015; 12: 196-207

22. Keeler AB, Suo D, Park J et al: Delineating neurotrophin-3 dependent signaling pathways underlying sympathetic axon growth along intermediate targets. *Mol Cell Neurosci*, 2017; 82: 66–75
23. Kim JY, Roh JK, Lee SK et al: Neurotrophin receptor immunoreactivity in severe cerebral cortical dysplasia. *Epilepsia*, 2002; 43(Suppl. 5): 220–26
24. Han F, Huo Y, Huang CJ et al: MicroRNA-30b promotes axon outgrowth of retinal ganglion cells by inhibiting Semaphorin3A expression. *Brain Res*, 2015; 1611: 65–73
25. Kim JE, Kim SM, Ahn SW et al: Brain abnormalities in neuromyelitis optica. *J Neurol Sci*, 2011; 302(1–2): 43–48
26. Matthews L, Marasco R, Jenkinson M et al: Distinction of seropositive NMO spectrum disorder and MS brain lesion distribution. *Neurology*, 2013; 80(14): 1330–37
27. Blanc F, Noblet V, Jung B et al: White matter atrophy and cognitive dysfunctions in neuromyelitis optica. *PLoS One*, 2012; 7(4): e33878
28. Pache F, Zimmermann H, Finke C et al: Brain parenchymal damage in neuromyelitis optica spectrum disorder – A multimodal MRI study. *Eur Radiol*, 2016; 26(12): 4413–22
29. Chen DW, Xu J, Liu W et al: Magnetic resonance imaging characteristics and clinical manifestations of brain abnormalities in neuromyelitis optica. *Zhonghua Shenjing Yixue Zazhi*, 2009; 8(8): 825–31
30. Wang F, Liu YO, Duan YY et al: Brain MRI manifestations of neuromyelitis optica. *Zhongguo Yixue Yingxiang Jishu*, 2015; 3: 336–39
31. Stromnes IM, Cerretti LM, Liggitt D et al: Differential regulation of central nervous system autoimmunity by T(H)1 and T(H)17 cells. *Nat Med*, 2008; 14(3): 337–42
32. Hosokawa T, Nakajima H, Doi Y et al: Increased serum matrix metalloproteinase-9 in neuromyelitis optica: Implication of disruption of blood-brain barrier. *J Neuroimmunol*, 2011; 236(1–2): 81–86
33. Tasaki A, Shimizu F, Sano Y et al: Autocrine MMP-2/9 secretion increases the BBB permeability in neuromyelitis optica. *J Neurol Neurosurg Psychiatry*, 2014; 85(4): 419–30
34. Uzawa A, Mori M, Masuda S et al: Markedly elevated soluble intercellular adhesion molecule 1, soluble vascular cell adhesion molecule 1 levels, and blood-brain barrier breakdown in neuromyelitis optica. *Arch Neurol*, 2011; 68(7): 913–17